

# Gradient-search phase-retrieval algorithm for inverse synthetic-aperture radar

James R. Fienup, FELLOW SPIE  
Environmental Research Institute of  
Michigan  
Optical & IR Science Laboratory  
P.O. Box 134001  
Ann Arbor, Michigan 48113-4001  
E-mail: fienup@erim.org

**Abstract.** We describe a new algorithm for correcting phase errors in synthetic-aperture radar data. It employs a gradient-search algorithm to minimize the energy of the image outside a support constraint. We give analytic expressions for the gradient of the error metric with respect to a point-by-point description of the phase error and with respect to the coefficients of a polynomial expansion of the phase error. These analytic gradients greatly speed the computations for the algorithm. We demonstrate successful phase-error correction for an image of a CV-580 aircraft collected with ERIM's Ground-to-Air Imaging Radar.

*Subject terms:* digital image recovery and synthesis; phase errors; synthetic-aperture radar; phase retrieval; image reconstruction; gradient search; motion errors; motion compensation; support constraint.

*Optical Engineering* 33(10), 3237-3242 (October 1994).

## 1 Introduction

When an inverse synthetic-aperture radar (ISAR) system is used to image a moving target, unknown motions of the target induce phase errors that cause a smearing of the image. Several algorithms are available for correcting phase errors. Algorithms for correcting higher-order phase errors usually depend on an isolated prominent point on the target. However, for some targets there may be no suitable prominent points on which to base a focusing algorithm. Then an algorithm not relying on prominent points is required to form a well-focused image.

A class of algorithms referred to as "phase-retrieval" algorithms can correct phase errors without the need for prominent points. They instead depend on knowledge of the *support* of the target (i.e., its spatial extent). This paper describes a phase-retrieval algorithm that finds a phase-error correction that minimizes the energy outside a support constraint. It uses a gradient-search nonlinear optimization technique that employs an analytically defined gradient with respect to either a point-by-point description of the phase-error function or a polynomial expansion of it. We show the effectiveness of the algorithm for an image of a CV-580 aircraft using ERIM's Ground-to-Air Imaging Radar (GAIR). In this case we roughly know the outline of the object and wish to determine its interior detail.

## 2 Model

We assume that the signal history (phase history) experiences phase errors  $\phi_e(u, v)$ , so that instead of the ideal signal history  $F(u, v)$ , we measure the aberrated signal history

$$\tilde{G}_0(u, v) = \tilde{F}(u, v) \exp[i\phi_e(u, v)] , \quad (1)$$

where  $u$  is the frequency (fast time) coordinate and  $v$  is the azimuth (slow time) coordinate. Although more generally  $\phi_e(u, v)$  is a 2-D phase error, in many circumstances it is well approximated as a 1-D phase error  $\phi_e(v)$ , a function of azimuth only. The phase error in radians is  $4\pi r(v)/\lambda$ , where  $r(v)$  is the instantaneous distance from the SAR to a reference point on the target, and  $\lambda$  is the center wavelength. The other dimension of the phase error is usually proportional to the absolute frequency ( $u$  plus the center frequency). For simplicity we will restrict our attention in what follows to 1-D phase errors only. This is appropriate for rigid-body translational motion in the plane of apparent rotation. The phase-retrieval approach can be generalized to 2-D phase errors.

The model above is appropriate only for spatially invariant phase errors, as would be caused by translational motion of the target. Other motions, such as rotational acceleration, may cause spatially variant errors, such as formatting errors. Spatially variant errors require a more sophisticated algorithm for correction, and they are beyond the scope of what we are considering here.

Inverse Fourier-transforming the signal history  $\tilde{G}(u, v)$  in frequency/range yields the range-compressed signal history

$$G_0(x, v) = F(x, v) \exp[i\phi_e(v)] , \quad (2)$$

where  $x$  is the range coordinate.

The target may have traveled through several range bins during the aperture time. In that case we should translate each pulse  $G_0(x, v)$  by an appropriate distance  $\Delta x(v)$  in range to align it with the neighboring pulses. We can find this distance by locating the peak of the cross-correlation of  $|G_0(x, v)|$  with  $|G_0(x, v-1)|$ . Using upsampling of the peak, and fitting a quadratic cap to the peak, we can easily determine this distance with fractional-pixel accuracy.

Paper DIR-03 received Jan. 31, 1994; revised manuscript received May 16, 1994; accepted for publication May 16, 1994. This paper is a revision of a paper presented at the SPIE conference Digital Image Recovery and Synthesis II, July 1993, San Diego, CA. The paper presented there appears (unrefereed) in SPIE Proceedings Vol. 2029.  
© 1994 Society of Photo-Optical Instrumentation Engineers. 0091-3286/94/\$6.00.

Performing a length- $N$  inverse FFT in azimuth of the range-aligned  $G_0(x, v)$  yields the image

$$g_0(x, y) = \mathcal{F}^{-1}[G_0(x, v)] = N^{-1} \sum_y G_0(x, v) \exp\left(\frac{i2\pi v y}{N}\right) \\ = f(x, y) * c(y) , \quad (3)$$

where  $\mathcal{F}$  is an azimuth Fourier transform,  $f(x, y)$  is the diffraction-limited image,  $c(y)$  is the azimuth impulse response, and all summations are over  $0, 1, \dots, N-1$  unless explicitly given otherwise. Our goal is to reconstruct  $f(x, y)$  from the smeared image  $g_0(x, y)$  or, equivalently,  $F(x, v)$  from  $G_0(x, v)$  by determining the phase error  $\phi_e(v)$  and subtracting it from the phase of  $G_0(x, v)$ .

### 3 Phase-Correction Algorithms

We can use any of several different phase-retrieval algorithms to solve this problem. For example, with the traditional iterative transform algorithm,<sup>1</sup> we iteratively transform (FFT) back and forth between the signal history domain, where we reinforce the magnitude of the signal history, and the image domain, where we reinforce the support constraint, until we arrive at a Fourier-transform pair that simultaneously satisfies both sets of constraints. The traditional iterative transform algorithm is designed to correct fully two-dimensional phase errors and does not take advantage of the 1-D nature of the phase error. We can do so by a gradient-search algorithm as described below. Gradient-search phase-retrieval algorithms were invented some time ago<sup>1</sup>; they have recently been generalized and have demonstrated good results when determining the aberrations of the Hubble Space Telescope (HST).<sup>2,3</sup> For the ISAR problem the algorithm is significantly different, however.

#### 3.1 Gradient-Search Algorithms Using Image-Support Error Metric

Our objective is to minimize the image-domain error metric

$$E_0 = \sum_{x, y \notin S} |g(x, y)|^2 = \sum_{x, y} [1 - S(x, y)] |g(x, y)|^2 , \quad (4)$$

where  $S(x, y)$  is unity within the image-support constraint and zero outside it. We define our current estimate of the (range compressed) signal history as

$$G(x, v) = G_0(x, v) \exp[-i\phi(v)] , \quad (5)$$

where  $G_0(x, v)$  is the measured signal history and  $\phi(v)$  is our current estimate of the phase error  $\phi_e(v)$ . Let  $p$  be an unknown parameter of  $G(x, v)$ . Then

$$\frac{\partial E_0}{\partial p} = \sum_{x, y} [1 - S(x, y)] g^*(x, y) \frac{\partial g(x, y)}{\partial p} + \text{c.c.} , \quad (6)$$

where c.c. stands for the complex conjugate of the term that precedes it, and

$$\frac{\partial g(x, y)}{\partial p} = N^{-1} \sum_v \exp\left(\frac{i2\pi v y}{N}\right) \frac{\partial G(x, v)}{\partial p} . \quad (7)$$

We readily see that for  $p$  representing a parameter of the phase-error estimate,

$$\frac{\partial G(x, v)}{\partial p} = -iG(x, v) \frac{\partial \phi(v)}{\partial p} . \quad (8)$$

Inserting Eqs. (7) and (8) into Eq. (6) yields

$$\frac{\partial E_0}{\partial p} = \sum_{x, y} [1 - S(x, y)] g^*(x, y) N^{-1} \\ \times \sum_{v'} \exp\left(\frac{i2\pi v' y}{N}\right) (-i)G(x, v') \frac{\partial \phi(v')}{\partial p} + \text{c.c.} \\ = -iN^{-1} \sum_x \sum_{v'} G_\gamma^*(x, v') G(x, v') \frac{\partial \phi(v')}{\partial p} + \text{c.c.} \\ = 2N^{-1} \sum_{v'} \frac{\partial \phi(v')}{\partial p} \sum_x \text{Im}[G_\gamma^*(x, v') G(x, v')] , \quad (9)$$

where

$$g_\gamma(x, y) = [1 - S(x, y)] g(x, y) \quad (10)$$

and  $G_\gamma(x, v) = \mathcal{F}[g_\gamma(x, y)]$ .

#### 3.2 Gradient with Respect to Phase-Function Values

First we consider minimizing over a point-by-point description of the unknown phase error in the signal history domain. If the parameter  $p$  is a sample value of the phase-error estimate  $\phi(v)$ , then

$$\frac{\partial \phi(v')}{\partial \phi(v)} = \delta(v, v') , \quad (11)$$

where  $\delta$  is the Kronecker delta function. Inserting this into Eq. (9) and performing the  $v'$  summation yields

$$\frac{\partial E_0}{\partial \phi(v)} = 2N^{-1} \sum_x \text{Im}[G_\gamma^*(x, v) G(x, v)] . \quad (12)$$

This is the gradient of the error metric with respect to a point-by-point description of the phase-error function.

All the partial derivatives that make up the gradient of  $E_0$  with respect to  $\phi(v)$  can be computed by two FFTs (actually, two sets of FFTs, each set consisting of  $N$  length- $N$  1-D FFTs, which together cost half the computations of a single 2-D FFT), the product to compute  $g_\gamma(x, y)$ , and the summation over  $x$  of  $\text{Im}[G_\gamma^*(x, v) G(x, v)]$ . The terms  $\text{Im}[G_\gamma^*(x, v) G(x, v)]$  are the contribution to the derivative of the error metric for each of the range bins.

#### 3.3 Gradient with Respect to Polynomial Coefficients

Using the same definition of the error metric  $E_0$  given above, we can minimize it with respect to the coefficients of a polynomial expansion of the phase error. Let

$$\phi(v) = \sum_{j=1}^J a_j L_j(v) , \quad (13)$$

where  $L_j(v)$  is the  $j$ 'th polynomial and  $a_j$  is its coefficient. A logical choice of polynomials would be normalized Legendre polynomials that are orthonormal over an interval. The unnormalized Legendre polynomials are given by

$$P_0(v) = 1, \quad (14)$$

$$P_1(v) = v, \quad (15)$$

and the remaining polynomials can be computed by the recursion relationship

$$P_n(v) = \frac{2n-1}{n} v P_{n-1}(v) - \frac{n-1}{n} P_{n-2}(v). \quad (16)$$

The Legendre polynomials that are scaled to be orthonormal over the interval  $[-1, 1]$  are given by

$$L_n(v) = \left( \frac{2N+1}{2} \right)^{1/2} P_n(v). \quad (17)$$

The interval over which the polynomial is normalized should ideally be scaled to correspond to the width of the nonzero signal history (i.e., not including any zero-pad area). Since

$$\frac{\partial \Phi(v)}{\partial a_j} = L_j(v), \quad (18)$$

we have

$$\begin{aligned} \frac{\partial E_0}{\partial a_j} &= 2N^{-1} \sum_v L_j(v) \sum_x \text{Im}[G_\gamma^*(x,v)G(x,v)] \\ &= \sum_v L_j(v) \frac{\partial E_0}{\partial \Phi(v)}. \end{aligned} \quad (19)$$

Note that this gradient requires all the same computations as the gradient with respect to  $\Phi(v)$ , plus an additional projection operation—the summation over  $v$  that we must perform for each of the  $J$  polynomial coefficients.

Based on our experience with the HST problem,<sup>2,3</sup> we hypothesize that the best procedure will be to minimize the image-domain error by the following steps:

1. Perform a polynomial-fitting gradient search of the phase error. Start with a low-order fit (say,  $J=2$  to 4), and then on that result perform a higher-order fit (say,  $J=10$  to 20).
2. Evaluate the phase-error function from the polynomial coefficients, and, starting with that result, perform a point-by-point phase-error-function gradient search.

### 3.4 Gradient with Respect to Fourier Coefficients

One final parameterization of the phase error that we will consider is a particular case of polynomials, namely Fourier series. This will be of great interest if the target has a sinusoidally varying position (e.g., a vibration). Furthermore, as we will see, the Fourier case has computational advantages. The Fourier series expansion of the phase function is

$$\Phi(v) = \sum_y \Phi(y) \exp\left(\frac{i2\pi v y}{N}\right), \quad (20)$$

where  $\Phi(y) = a(y) + ib(y)$ , a complex number, is the coefficient of the  $y$ 'th Fourier kernel. Since by definition  $\Phi(v)$  is a real-valued function,  $a(y)$  must be even,  $b(y)$  odd, and  $\Phi(y)$  Hermitian when we define the interval of  $y$  to be symmetric about the origin. Choosing the parameter  $p$  to be  $a(y)$  or  $b(y)$ , we have

$$\frac{\partial \Phi(v)}{\partial a(y)} = 2 \cos\left(\frac{2\pi v y}{N}\right) \quad (21)$$

and

$$\frac{\partial \Phi(v)}{\partial b(y)} = -2 \sin\left(\frac{2\pi v y}{N}\right), \quad (22)$$

where we have used the symmetry properties  $a(-y) = a(y)$  and  $b(-y) = -b(y)$ . Therefore we have

$$\frac{\partial E_0}{\partial a(y)} = 4N^{-1} \sum_v \cos\left(\frac{2\pi v y}{N}\right) \sum_x \text{Im}[G_\gamma^*(x,v)G(x,v)]. \quad (23)$$

Letting

$$H(v) = \sum_x G_\gamma^*(x,v) G(x,v), \quad (24)$$

we have

$$\begin{aligned} \frac{\partial E_0}{\partial a(y)} &= 4N^{-1} \sum_v \cos\left(\frac{2\pi v y}{N}\right) \text{Im}[H(v)] \\ &= 2 \text{Im}[h(y) + h(-y)], \end{aligned} \quad (25)$$

where  $h(y) = \mathcal{F}^{-1}[H(v)]$ ; and similarly

$$\frac{\partial E_0}{\partial b(y)} = 2 \text{Re}[h(y) - h(-y)]. \quad (26)$$

This gradient requires three FFTs (two to compute  $G_\gamma$  and one to compute  $h$ ), but avoids the separate summation for each polynomial coefficient that the Legendre (or other) polynomials require. Therefore it will be faster when using a large number of (Fourier) polynomial coefficients.

### 3.5 Support Constraint

One should take special care to define a support constraint as well as possible. The support constraint should be as tight (small) as possible while still including all the mainlobe returns from the target. If the support constraint is much too large, then the algorithm tends to stagnate without correcting the phase error. If the support constraint is too small, then the algorithm will inadvertently try to truncate true parts of the image, and it may perform poorly. Take care to include within the support constraint any returns from vibrating or rotating parts of the target (such as a propeller) that are Doppler shifted (in azimuth) away from the target proper. Define  $S(x,y) = 1$  over an azimuth extent that includes the Doppler-shifted returns in those range bins. If we know that a whole range bin is unreliable, we can exclude it from the definition of the error metric (and from the computation of the gradient) by defining  $S(x,y) = 1$  over the entire azimuth extent of the array for those range bins. We would, however, correct those

range bins according to the phase-error estimate. If we do not know the support constraint *a priori*, then we can at least determine upper bounds on it from the support of the autocorrelation function,<sup>4</sup> which we can compute from the given data.

### 3.6 Gradient Search

Given the definition of the error metric  $E_0$  and the analytic expressions for the gradient of the error metric derived above, we used standard gradient-search routines to estimate the phase error. We obtained similar reconstruction results using MATLAB-based software (using the `fminu` minimizer,<sup>5</sup> which employs a Broydon-Fletcher-Goldfarb-Shanno quasi-Newton method with a mixed quadratic and cubic line search procedure) and a C program (using the `fprmn` optimizer from

*Numerical Recipes*,<sup>6</sup> which is a Fletcher-Reeves-Polak-Ribiere minimizer).

## 4 Examples of Results

Figure 1 shows an example of applying the phase-retrieval algorithm to an image collected by ERIM's Ground-to-Air Imaging Radar (GAIR).<sup>7</sup> We started with a well-focused  $512 \times 512$  image of ERIM's CV580 aircraft, as shown in Fig. 1(a). Focusing was provided using motion data from an on-board inertial measurement unit. We then Fourier-transformed the image back to the signal history domain, added a synthetic phase error, and then inverse Fourier-transformed back to the image domain to obtain the image shown in Fig. 1(b), which is smeared by the synthetic phase error. The phase error we added is a fifth-order polynomial

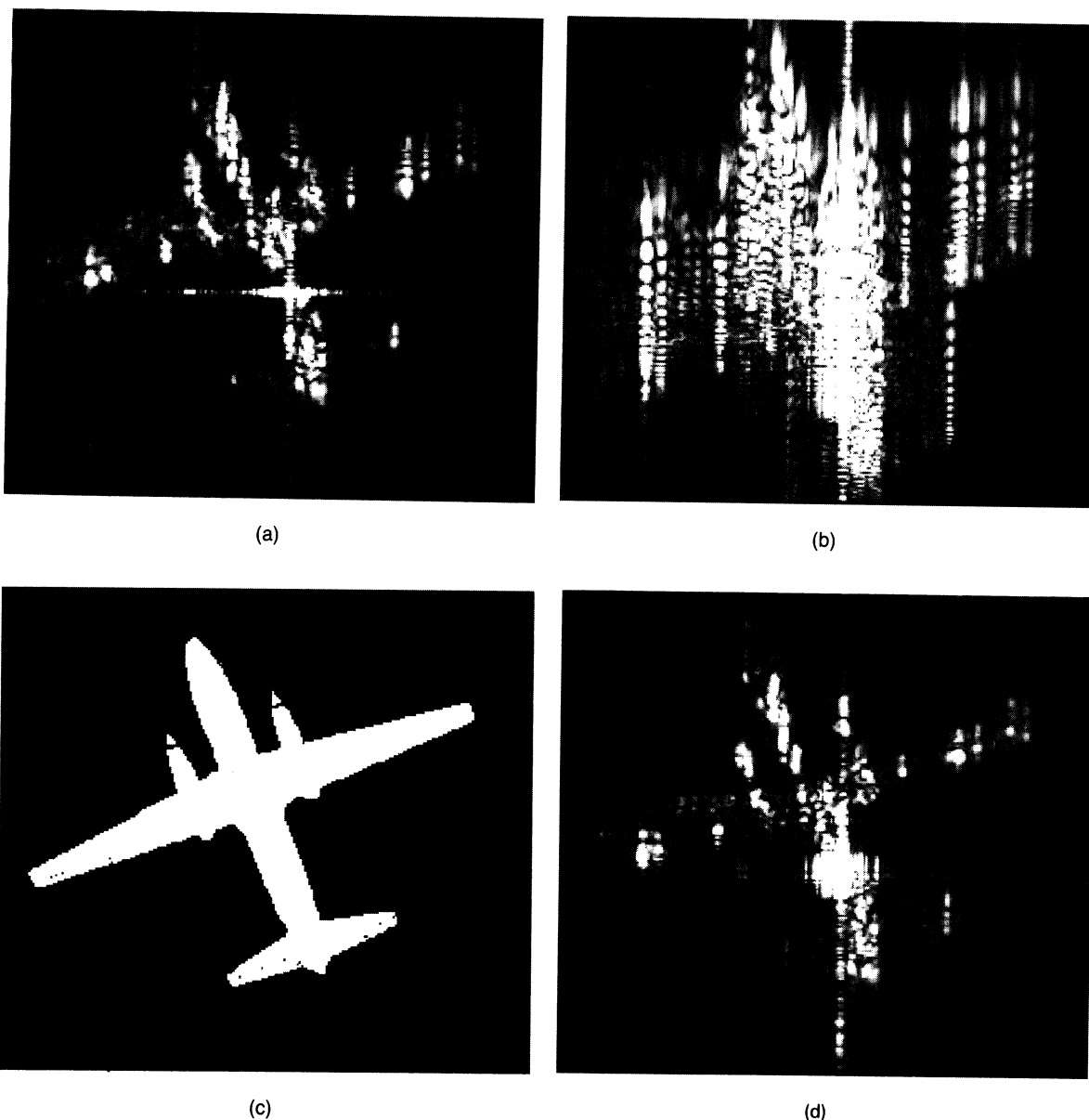


**Fig. 1** Image-correction result: (a) original focused image, (b) image smeared by fifth-order synthetic phase errors, (c) support constraint and (d) image corrected using phase-retrieval algorithm.

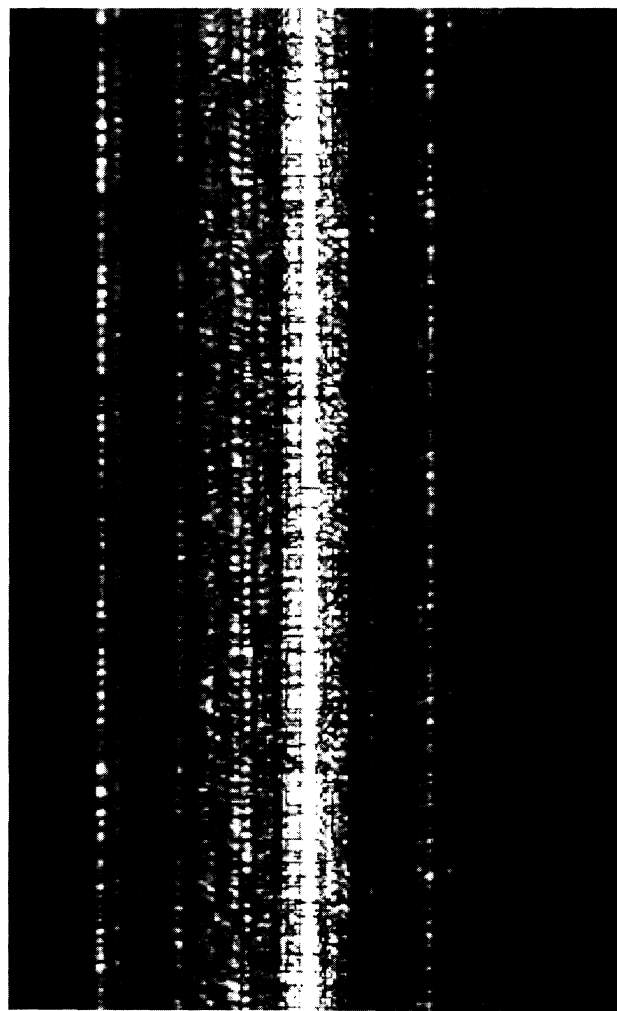
having an integrated phase error of 4.1 rad rms. Knowing the orientation of the aircraft, we obtained the support constraint required by the phase-retrieval algorithm from a CAD/CAM model of the target, as shown in Fig. 1(c). The smeared image shown in Fig. 1(b) was the starting point for our phase-retrieval algorithm. We used the polynomial coefficient version of the algorithm, using five coefficients, all initially valued zero. Figure 1(d) shows the image corrected by the phase-retrieval algorithm. It is considerably less smeared than the given smeared image, and is of quality comparable to that of the original focused image. In fact, the wings appear better focused than in the original, whereas the tail appears more poorly focused, indicating that part of the smearing is due to a spatially variant error. Since the phase-retrieval algorithm only attempts to correct spatially invariant phase errors, it cannot perfectly focus all parts of this image simultaneously.

Figure 2 shows a second example. In this case we went back to the original signal history by adding to the corrected signal history the phase error that was previously removed according to the motion estimate obtained from the on-board inertial measurement unit. The phase error was huge: 2800 rad (max - min) over 350 samples. This image, which is completely smeared in azimuth, as shown in Fig. 2(a), is what we would ordinarily obtain without information from an on-board inertial measurement unit. The algorithm initially stagnated when given this image. We overcame the stagnation problem by first performing a crude focusing. We tried several different quadratic phase errors, each differing by  $\pm 200$  rad, and chose the quadratic phase correction causing the sharpest image. This works because a large component of the phase error is indeed quadratic. We measure sharpness by spatially summing over the square of the image intensity. Then we continued with the phase-retrieval algorithm, using the point-by-point phase-function model, which no longer stagnated. Figure 2(b) shows the reconstructed image. (For this particular image, shear averaging<sup>8</sup> also worked very well.)

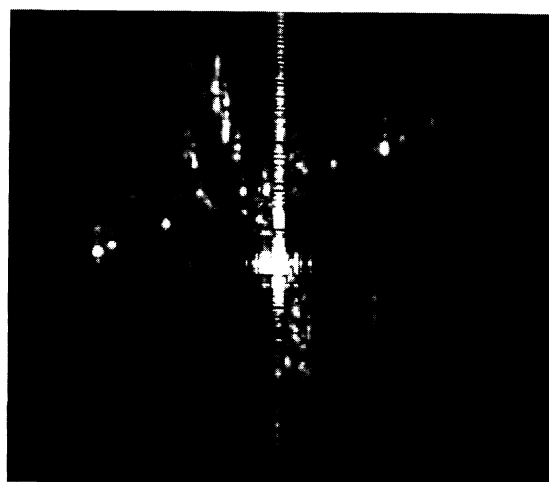
We performed experiments to determine the sensitivity of the algorithm to the quality of the support constraint. To the correct support constraint we added  $n$  pixels all around its perimeter, making it  $2n$  pixels too large in diameter. We found that for  $n = 0$  to 4 we obtained results similar to those shown in the figures. When  $n = 8$ , the phase-error estimate stayed too close to the original estimate and the image would tend to fill the support constraint. Since the energy Doppler-shifted outside the support constraint by the propellers was a small fraction of the total energy, including that energy in the error metric degraded the reconstructed image only slightly.

## 5 Conclusions

We have developed a phase-retrieval algorithm, using a support constraint, for correcting phase errors in synthetic-aperture radar data. We have derived analytic expressions for the gradient of an error metric with respect to phase-error parameters. This allows for efficient computation of the gradient, which is used by a standard nonlinear optimization algorithm. We have shown good reconstruction results with actual SAR data. The results demonstrate that the phase-retrieval approach can correct phase errors and reduce image smearing due to unknown target motion. However, the algorithm can also get stuck in a local minimum and fail to



(a)



(b)

**Fig. 2** Second image-correction result: (a) image smeared by phase errors induced by target motion and (b) image corrected using phase-retrieval algorithm. The support constraint is the same as in Fig. 1.

converge to the correct image. In this case multiple applications of the algorithm using different initial starting guesses for the phase error can overcome this problem. If large quadratic phase errors are present, then it helps to remove that component first.

If a bright, isolated prominent point is available, then it is best to use it to focus the image; and if multiple prominent points are available, then we can correct for space-variant errors as well.<sup>9,10</sup> However, when a prominent point is not available, and if one has a reasonably good estimate of the support of the image, then a phase-retrieval algorithm using a support constraint can work when other approaches fail. Alternatively, the phase-retrieval algorithm can be one step in a multiple-step image reconstruction procedure.

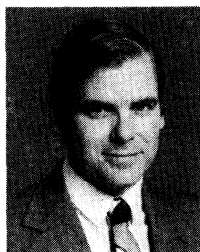
This phase-retrieval algorithm, based on a support constraint, is most useful for the special case in which we know *a priori*, at least roughly, the outline of the object, and we wish to reconstruct the interior details of the image. It may also be useful when the support constraint is derived from the measured data.<sup>4</sup>

### Acknowledgment

The author thanks Joy VanBuhler for successfully implementing the C-code version of the algorithm and producing reconstruction results.

### References

1. J. R. Fienup, "Phase retrieval algorithms: a comparison," *Appl. Opt.* **21**, 2758–2769 (1982).
2. J. R. Fienup, "Phase retrieval algorithms for a complicated optical system," *Appl. Opt.* **32**, 1737–1746 (1993).
3. J. R. Fienup, J. C. Marron, T. J. Schulz, and J. H. Seldin, "Hubble Space Telescope characterized by using phase retrieval algorithms," *Appl. Opt.* **32**, 1747–1768 (1993).
4. T. R. Crimmins, J. R. Fienup, and B. J. Thelen, "Improved bounds on object support from autocorrelation support and application to phase retrieval," *J. Opt. Soc. Am. A* **7**, 3–13 (1990).
5. A. Grace, *Optimization Toolbox User's Guide*, pp. 2–19, Math Works, Natick, MA (1990).
6. W. H. Press et al., *Numerical Recipes in C*, p. 321, Cambridge Univ. Press (1988).
7. R. Goodman, W. Nagy, J. Wilhelm, and S. Crippen, "A high fidelity ground to air imaging radar system," in *Proc. IEEE 1994 National Radar Conference* (Mar. 1994).
8. J. R. Fienup, "Phase error correction by shear averaging," in *Signal Recovery and Synthesis III*, pp. 134–137, OSA (1989).
9. S. A. Werness, M. A. Stuff, and J. R. Fienup, "Two dimensional imaging of moving targets in SAR data," in *24th Asilomar Conf. on Signals, Systems and Computing* (Nov. 1990).
10. S. A. Werness, W. G. Carrara, L. Joyce, and D. Franczak, "Moving target imaging algorithm for SAR data," *IEEE Trans. Aerospace Electron. Systems* **26**, 57–67 (1990).
11. J. R. Fienup, "Phase retrieval algorithm for inverse synthetic aperture radar," in *Digital Image Recovery and Synthesis II, Proc. SPIE 2029*, 63–67 (July 1993).



**James R. Fienup** received BA degrees in physics and mathematics (magna cum laude) from Holy Cross College, Worcester, Massachusetts, in 1970, and the MS and PhD degrees in applied physics from Stanford University in 1972 and 1975, respectively. He was a National Science Foundation graduate fellow from 1970 to 1972. He is currently the Senior Scientist in the Optical & IR Science Laboratory of the Environmental Research Institute of

Michigan, which he joined in 1975. His research activities include phase retrieval and image reconstruction, optical and digital image processing for synthetic-aperture radar, and holographic optical elements. His publications include more than 90 papers, and he has three patents. He is a fellow of SPIE and of the Optical Society of America, and is a senior member of the IEEE. He is the recipient of the SPIE 1979 Rudolph Kingslake Medal and Prize, the International Commission for Optics 1983 International Prize in Optics, and the Best Paper Award for 1990 by the IRIS Specialty Group on Active Imaging. He has cochaired SPIE symposia. He has served as associate editor of *Optics Letters*, three times as a feature editor of the *Journal of the Optical Society of America A*, and on NASA's Hubble Space Telescope Image Processing Working Group.